Draft version February 19, 2024
Typeset using LaTeX default style in AASTeX61

arXiv:1805.08075v1 [astro-ph.GA] 18 May 2018

AN APPROACH TO ESTIMATE THE BINDING ENERGY OF INTERSTELLAR SPECIES

Ankan Das,[1] Milan Sil,[1] Prasanta Gorai,[1] Sandip K. Chakrabarti,[2,1] and J. C. Loison[3]

[1] *Indian Centre for Space Physics, 43 Chalantika, Garia Station Road, Kolkata 700084, India*
[2] *S. N. Bose National Centre for Basic Sciences, Salt Lake, Kolkata 700106, India*
[3] *Institute of Molecular Sciences, University of Bordeaux, CNRS UMR 5255, France*

ABSTRACT

One of the major obstacles to accurately model the interstellar chemistry is an inadequate knowledge about the binding energy (BE) of interstellar species with dust grains. In denser region of molecular cloud, where very complex chemistry is active, interstellar dust is predominantly covered by H_2O molecules and thus it is essential to know the interaction of gas phase species with water ice to trace realistic physical and chemical processes. To this effect, we consider water (cluster) ice to calculate the BE of several atoms, molecules, and radicals of astrochemical interest. Systematic studies have been carried out to come up with a relatively more accurate BE of astrophysically relevant species on water ice. We increase the size of the water cluster methodically to capture the realistic situation. Sequentially one, three, four, five and six water molecules are considered to represent water ice analogue in increasing order of complexity. We notice that for most of the species considered here, as we increase the cluster size, our calculated BE value starts to converge towards the experimentally obtained value. More specifically, our computed results with water c-pentamer (average deviation from experiment $\sim \pm 15.8\%$) and c-hexamer (chair) (average deviation from experiment $\sim \pm 16.7\%$) configuration are found to be more nearer as the experimentally obtained value than other water clusters considered.

Keywords: Astrochemistry, ISM: atoms ISM: molecules – molecular processes, ISM: dust, Methods: numerical

Corresponding author: Ankan Das
ankan.das@gmail.com

1. INTRODUCTION

Molecules in space are synthesized via gas-phase reactions as well as the reactions occurring on interstellar grain surfaces. In the process of chemical enrichment, gas and grains continuously exchange their chemical components with each other. Interstellar dust act similar to a catalyst (Garrod & Herbst 2006; Herbst & Van Dishoeck 2009) during the chemical enrichment of the interstellar medium (ISM). Knowledge of the binding energies (BE) of the interstellar species is very crucial to understand synthesis of molecules in the gas phase as well as interstellar icy grain mantle. Species which are being produced or trapped on interstellar ice may transfer to gas phase by various desorption mechanism such as non-thermal reactive desorption (Garrod et al 2007) (efficient desorption mechanism at low temperature), thermal desorption (efficient at high temperature) and energetic processes such as, direct or indirect photo evaporation by photon or cosmic ray particles. Interestingly, all the parameters causing desorption are directly or indirectly related to the BE of the species (Gorai et al. 2017a,b; Sil et al. 2018). According to Minissale & Dulieu (2014), the efficiency of non-thermal chemical desorption mechanism basically depends on four parameters: enthalpy of formation, degrees of freedom, BE and mass of newly formed molecules. Minissale et al. (2016) proposed a new chemical desorption equation by relating the equipartition of energy. Recently, Wakelam et al. (2017) studied the efficiency of chemical desorption for a new set of BEs by including both the chemical desorption rates proposed by Garrod et al (2007) and Minissale et al. (2016).

Since 1990s Temperature Programmed Desorption (TPD) technique is used to experimentally determine the BE values. Although TPD measures the desorption energy, this energy essentially is the binding energy of the species if there are no activated processes. Experimentally determined BE depends on the nature of substrate from which the species desorb and on several other parameters like the property of the deposited ices (i.e., pure, mixed, or layered). These parameters has an effect on the obtained BE values from TPD experiments. But with the TPD method, it is quite difficult to provide the BE values of the radicals because of their short life under the laboratory conditions. However, above 40 K, the mobility of the radicals exponentially increased and can actively take part in controlling the surface chemistry. In order to map the chemical composition in the intermediate temperature ($40 - 80$ K) regime, it is essential to have an estimation of the BE of these radicals. To this effect, parametric computational studies can provide faster information as compared to experimental studies. Prior to the era of TPD experiments, some estimated values of BE were used in gas-grain chemical models (Tielens & Hagen 1982; Hasegawa & Herbst 1993; Charnley 1997). These estimations were based on the polarizability of molecules or atoms, which provides an estimate of strength of van der Waals interaction with a bare grain surface. Silicate and carbonaceous type grains are abundant in the ISM. However, denser regions of molecular clouds are predominantly composed of H_2O in amorphous phase with addition of some other impurities, such as CO, CO_2, NH_3, CH_4, H_2CO and CH_3OH etc. Though early experiments (Chakarov & Kasemo 1998) and astronomical observations (Malfait et al. 1998; Maldoni et al. 2003) clearly suggest the presence of crystalline ice, vapor-deposited amorphous ice (also called amorphous solid water, ASW) continues to attract more fundamental researchers due to its occurrences in astronomical environments such as icy satellites, comets, planetary rings and interstellar grains etc. Various surface processes such as adsorption, diffusion, tunneling reactions, and nuclear-spin conversion on interstellar ASW are summarized in Hama & Watanabe (2013). ASW is by far the largest component of the icy mantles, with abundances of $\sim 10^{-4}$ with respect to the total hydrogen (Williams & Herbst 2002), equivalent to coverages of up to 100 mono-layers (ML). The extinction threshold (A_V) for H_2O mantle is ~ 3.3 mag (Whittet et al. 1988). It should be kept in mind that interstellar ices are thought to have low levels of porosity, as they are continuously exposed to external radiation (Palumbo 2006).

The BE or adsorption energy of various species are the essential input parameters for interstellar gas-grain chemistry but only a few have been obtained experimentally. Among the experimentally obtained BE values, most of the values were obtained from TPD experiments. Collings et al. (2004) presented an extensive TPD study for a collection of 16 astrophysically relevant molecular species. Ward et al. (2012) used TPD experiments coupled with time-of-flight mass spectrometry to determine the yield of OCS and additionally yields value for the computation of desorption energies of O atom and OCS. The interaction and auto-ionization of HCl on low-temperature ($80 - 140$ K) water ice surfaces has been studied by Olanrewaju et al. (2011) by using low-energy ($5 - 250$ eV) electron-stimulated desorption (ESD) and temperature programmed desorption (TPD). Dulieu et al. (2013) also performed TPD experiment to derive the BE of different species on the silicate substrate. Noble et al. (2012) present experimental study of the desorption of CO, O_2 and CO_2 from three different surfaces: non-porous ASW, crystalline ice and amorphous olivine-type silicate. Very

recently, Penteado et al. (2017) carried out a systematic study on the effects of uncertainties associated with the BE on the astrochemical two-phase model of a dark molecular cloud. They also pointed out the importance of branching ratios which need experimental validation and careful implementation in astrochemical model. They have estimated the binding energies (mentioned in the Appendix Table A1) based on the results presented in Collings et al. (2004) for the deposition of each species on a H_2O substrate as:

$$E_{bind,X} = \frac{T_{des,X}}{T_{des,H_2O}} \times E_{bind,H_2O} \tag{1}$$

where $T_{des,X}$ is the desorption temperature of species X deposited on a H_2O film, T_{des,H_2O} is the desorption temperature of H_2O, and E_{bind,H_2O} is the BE of H_2O.

Most of the neutral species, even H and H_2, can be physisorbed (barrier-less) onto ice mantles by the van der Waals force. Although the potential energy can develop a deep minimum in chemisorption, physisorption is more relevant for interaction with grain surface. In some cases, computational studies can help to derive BEs of the interstellar species. For example, Al-Halabi & van Dishoeck (2007) simulated adsorption of H atoms to ASW using classical trajectory calculations, the off-lattice kinetic Monte Carlo approach was used by (Karssemeijer & Cuppen 2014) to estimate the BE of CO and CO_2. To simulate the adsorption of H_2 with ASW and crystalline ice, classical trajectory (CT) calculations have been performed by Hornekr et al. (2005). Recently, Sil et al. (2017) performed quantum chemical calculations to determine BE of H and H_2 with astrophysical relevant surfaces. In the absence of any experimental or theoretical data, as a rule of thumb, BE of an unknown species is very crudely estimated by the addition of BEs of its reactants. But this assumption may lead to very misleading results. This motivates us to devise an approach to better approximate the BE for some relevant interstellar species.

In this paper, we present our computed BEs of 100 interstellar and circumstellar species where water cluster is used as an adsorbent. Detail comparison is also made between the calculated BEs and available experimental or theoretically obtained BE values. High-level quantum chemical calculations are performed to calculate the BEs of various species. This paper is organized as follows. In Section 2, we discuss computational details and methodology. In Section 3, results are discussed in detail and finally, concluding remark is made in Section 4.

2. COMPUTATIONAL DETAILS AND METHODOLOGY

The adsorption energy is usually seen as a local property arising from the electronic interaction between a solid support (grain surface or adsorbent) and the species deposited on its surface (adsorbate). We calculate the adsorption energy (BE) of a species on the grain surface as follows:

$$E_{ads} = E_{ss} - (E_{surface} + E_{species}) \tag{2}$$

where E_{ads} is the adsorption energy, E_{ss} is the optimized energy for a species placed at a suitable distance from the grain surface, $E_{surface}$ and $E_{species}$ are the optimized energies of the grain surface and species respectively. According to various studies, around dense cloud regions, water (H_2O) is the major ($\sim$70% by mass) constituent of a grain mantle (Keane et al. 2001; Das, Acharyya & Chakrabarti 2010; Das & Chakrabarti 2011; Das et al. 2016), and thus the incoming gas species may be directly adsorbed onto the water ice. So, a knowledge of the BE of the adsorbed species with water ice is essential to build a realistic astrochemical model which studies the composition of the interstellar grain mantle. For our investigation on the BEs, we use the most stable configurations of water monomer, c-trimer, c-tetramer, c-pentamer, and c-hexamer (chair) (Ohno et al. 2005) respectively as the adsorbents (Fig. 1).

We carry out all the calculations by using Gaussian 09 suite of programs developed by Frisch et al. (2013). Second order Møller-Plesset (MP2) method with aug-cc-pVDZ basis set is mainly used in computing the optimized energy of all the species and complexes. A prefix 'aug' is used to indicate the addition of diffuse function and cc-pVDZ, cc-pVTZ are the Dunnings correlation consistent basis set (Dunning Jr 1989) having the double and triple zeta function respectively. CCSD(T) (Coupled Cluster single-double and perturbative triple) method with aug-cc-pVTZ basis set is also used to calculate the single point energy by taking the optimized structure obtained with MP2 method for some tetramer and hexamer (water cluster) to check the dependency of our computed BE values on the implemented

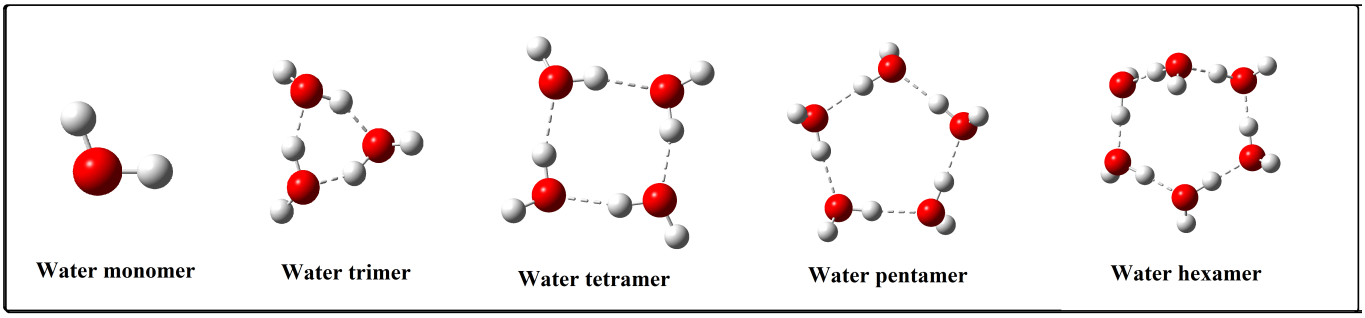


Figure 1. Configurations of water molecule(s) which are used in the present work.

method and basis set. Fully optimized ground state structure is verified to be a stationary point (having non-negative frequency) by harmonic vibrational frequency analysis and most of the calculations are performed without zero point energy (ZPE) and without basis set superposition error (BSSE) corrections. A study have also been carried out by including ZPE and excluding BSSE (using the Counterpoise method) to check their influence on calculated BE values.

3. RESULTS AND DISCUSSIONS OVER CALCULATED BINDING ENERGY VALUES

In this Section, results of high-level quantum chemical calculations are presented and discussed in detail. Wakelam et al. (2017) selected 16 stable species to compute the BEs by considering a water monomer. Here, we employ similar methodology and carry out calculations by increasing the cluster size to check its consequences. Five different sets of adsorbent are used to see the effects of cluster size on the computed BEs. With the increase in cluster size, we found an increasing trend of BEs for most of the species considered here. Most interestingly the calculated BEs by considering water c-pentamer and c-hexamer (chair) configuration seems to be closer to the experimentally obtained values as compared to that of the calculated BEs with the water monomer, c-trimer, or c-tetramer configurations. Binding energies of these 16 stable species with various water cluster configurations are given in Table 1. For the sake of comparison, in Table 1, we also show the experimentally obtained values, estimated values from Wakelam et al. (2017), and BEs from UMIST (`http://udfa.ajmarkwick.net`) database.

For most of the cases, Fig. 2 shows an increasing trend of BEs with the increase in the size of the water cluster as an adsorbent. Figure 2 is subdivided into 16 blocks for 16 different species. Along the X-axis, we show the size of water cluster and along Y-axis, we show the percentage deviation from the experimentally obtained values. The horizontal red line in each block denotes the zero deviation from experimental values. The result clearly shows that for most of the cases the percentage deviation between experiment and theory is comparatively higher (underestimated) when the water monomer is used and it is lower when c-pentamer or c-hexamer (chair) configuration of water is used as an absorbent. All the percentage deviations of each species are shown in parentheses of Table 1 and Table 2 as well. In order to check the overall comparison between our calculations and experimentally obtained values, we calculate the average absolute percentage deviation and root mean square fractional deviation of these species and these are also presented in Table 1 and Table 2. Figure 3 depicts the percentage deviation from experimental BE values of each species for water hexamer. It is striking to note that (in Table 1) while we sequentially increase the cluster size by considering water monomer, c-trimer, c-tetramer, c-pentamer and c-hexamer (chair) as a substrate, the average percentage deviations are found to be $\pm 41.6\%$, $\pm 24.6\%$, $\pm 18.8\%$, $\pm 15.8\%$, and $\pm 16.7\%$ respectively and fractional root mean square deviations are found to be 0.435, 0.324, 0.236, 0.205, and 0.221 respectively. These average absolute percentage deviations and fractional R.M.S. deviations are also shown in Fig. 4(a) and 4(b) respectively for a better understanding.

In Table 1, we also present the average percentage deviation of calculated BE values from Wakelam et al. (2017). We see that on an average, the predicted/scaled values of Wakelam et al. (2017) deviate the experimental values by $\pm 12.8\%$ while M06-2X method with aug-cc-pVTZ basis set was used and deviate the value by $\pm 11.7\%$ while MP2 method with aug-cc-pVTZ basis set was used. It is also shown that with respect to the experimental values noted in Table 1, BE values in UMIST database deviates the experimental values by $\pm 15.4\%$. Our calculation with c-pentamer and c-hexamer (chair) configuration are producing results (no fitting is required as in Wakelam et al.

Table 1. Calculated BEs Along with Some Frequently Used BEs for Astrochemical Modeling.

Sl. No.	Species	Calculated BE in Kelvin on different water clusters using MP2/aug-cc-pVDZ					Experimental values of BE	BE from Wakelam et al. (2017)		BE in Kelvin from
		Monomer 	Trimer 	Tetramer 	Pentamer 	Hexamer 	in Kelvin	in Kelvin using DFT M06-2X	in Kelvin using MP2 aug-cc-pVTZ	UMIST database[k]
1.	OCS	1139 (-53.1 %)	1905 (-21.6 %)	1571 (-35.3 %)	2014 (-17.1 %)	1808 (-25.5 %)	2430 ± 24[a]	2100 (13.5 %)	—	2888 (18.8 %)
2.	HCl	3116 (-39.7 %)	3545 (-31.4 %)	3924 (-24.1 %)	4099 (-20.7 %)	4104 (-20.6 %)	5172[b]	4800 (7.1 %)	5000 (-3.3 %)	900 (-82.5 %)
3.	CH_3CN	2676 (-42.8 %)	4108 (-12.2 %)	2838 (-39.3 %)	2820 (-39.7 %)	3786 (-19.1 %)	4680[c]	4300 (8.1 %)	4800 (2.5 %)	4680 (0.00 %)
4.	H_2O_2	3838 (-36.0 %)	3942 (-34.3 %)	3928 (-34.5 %)	5288 (-11.8 %)	5286 (-11.9 %)	6000[d]	6800 (-13.3 %)	6100 (1.6 %)	5700 (-5.0 %)
5.	CH_3OH	3124 (-37.5 %)	3924 (-21.5 %)	4368 (-12.6 %)	4607 (-7.8 %)	4511 (-9.7 %)	5000[e]	4800 (4.0 %)	4850 (-3.0 %)	4930 (-1.4 %)
6.	NH_3	3501 (-36.6 %)	3745 (-32.3 %)	3825 (-30.8 %)	3751 (-32.1 %)	5163 (-6.6 %)	5530[c]	5600 (-1.2 %)	5500 (-0.5 %)	5534 (0.6 %)
7.	CO	595 (-54.2 %)	664 (-48.9 %)	1263 (-2.8 %)	1320 (1.5 %)	1292 (-0.6 %)	1300[g]	1300 (0.0 %)	1100 (-15.3 %)	1150 (-11.5 %)
8.	C_2H_2	1532 (-40.7 %)	2581 (-0.2 %)	2593 (0.2 %)	2633 (1.7 %)	2640 (2.0 %)	2587[c]	2600 (-0.5 %)	2700 (4.3 %)	2587 (0.0 %)
9.	CO_2	1506 (-34.5 %)	1935 (-15.9 %)	2293 (-0.3 %)	2287 (-0.5 %)	2352 (2.2 %)	2300[g]	3100 (34.7 %)	2600 (13.0 %)	2990 (30.0 %)
10.	N_2	793 (-27.9 %)	884 (-19.6 %)	900 (-18.1 %)	893 (-18.8 %)	1161 (5.5 %)	1100[e]	1100 (0.0 %)	1400 (27.2 %)	790 (-28.1 %)
11.	NO	886 (-50.7 %)	568 (-68.4 %)	1265 (-29.7 %)	1300 (-27.7 %)	1988 (10.4 %)	1800[e]	1600 (11.1 %)	1700 (-5.5 %)	1600 (-11.1 %)
12.	O_2	391 (-67.4 %)	382 (-68.2 %)	940 (-21.6 %)	1116 (-7.0 %)	1352 (12.6 %)	1200[g]	1000 (16.6 %)	900 (-25.0 %)	1000 (-16.6 %)
13.	H_2S	1727 (-37.0 %)	2849 (3.9 %)	2556 (-6.8 %)	2396 (-12.6 %)	3232 (17.8 %)	2743[c,k]	2700 (1.5 %)	2550 (-7.0 %)	2743 (0.0 %)
14.	CH_3CCH	2266 (-9.3 %)	2580 (3.2 %)	2342 (-6.3 %)	2673 (6.9 %)	3153 (26.1 %)	2500 ± 40[h]	3800 (-52.0 %)	3800 (52.0 %)	2470 (-1.2 %)
15.	HNCO	2046 (-47.5 %)	3973 (1.9 %)	3922 (0.5 %)	4097 (5.0 %)	5554 (42.4 %)	3900[i]	4850 (-24.3 %)	—	2850 (-26.9 %)
16.	CH_4	469 (-51.2 %)	1066 (10.7 %)	1327 (37.7 %)	1366 (41.8 %)	1491 (54.8 %)	963[j]	800 (16.9 %)	1000 (3.8 %)	1090 (13.1 %)
Average absolute deviation		± 41.6 %	± 24.6 %	± 18.8 %	± 15.8 %	± 16.7 %		± 12.8 %	± 11.7 %	± 15.4 %
Fractional RMS deviation		0.435	0.324	0.236	0.205	0.221		0.189	0.182	0.254

Notes. Percentage deviation from experimental BE values (column 8) are shown in parentheses for columns 3, 4, 5, 6, 7, 9, 10 and 11.
[a] Ward et al. (2012), [b] Olanrewaju et al. (2011), [c] Collings et al. (2004), [d] Dulieu et al. (2013), [e] Wakelam et al. (2017), [g] Minissale et al. (2016), [h] Kimber et al. (2014), [i] Noble et al. (2015), [j] Raut et al. (2007), [k] UMIST database (`http://udfa.ajmarkwick.net`).

Table 2. Comparison of Calculated BEs Using Water Monomer (adsorbent) with Experimentally used BEs.

Sl. No.	Species	BE in Kelvin using different methods and basis sets including (+) or excluding (+) ZPE and BSSE					Experimental values of BE in Kelvin
		MP2/aug-cc-pVDZ - ZPE and - BSSE	MP2/aug-cc-pVDZ + ZPE but - BSSE	MP2/aug-cc-pVDZ - ZPE but + BSSE	MP2/aug-cc-pVTZ - ZPE and - BSSE	CCSD(T)/aug-cc-pVTZ - ZPE and - BSSE	
1.	OCS	1139 (-53.1 %)	683 (-71.9 %)	803 (-66.9 %)	1074 (-55.8 %)	1086 (-55.3 %)	2430 ± 24[a]
2.	HCl	3116 (-39.7 %)	2113 (-59.1 %)	2627 (-49.2 %)	2975 (-42.5 %)	2777 (-46.3 %)	5172[b]
3.	CH_3CN	2676 (-42.8 %)	1970 (-57.9 %)	2242 (-52.1 %)	2676 (-42.8 %)	2635 (-43.7 %)	4680[c]
4.	H_2O_2	3838 (-36.0 %)	2647 (-55.9 %)	3204 (-46.6 %)	3775 (-37.1 %)	3802 (-36.6 %)	6000[d]
5.	CH_3OH	3124 (-37.5 %)	2149 (-57.0 %)	2586 (-48.3 %)	3021 (-39.6 %)	2988 (-40.2 %)	5000[e]
6.	NH_3	3501 (-36.6 %)	2368 (-57.2 %)	2941 (-46.8 %)	3375 (-39.0 %)	3332 (-39.7 %)	5530[c]
7.	CO	595 (-54.2 %)	236 (-81.8 %)	349 (-73.2 %)	565 (-56.5 %)	662 (-49.1 %)	1300[g]
8.	C_2H_2	1532 (-40.7 %)	950 (-63.3 %)	1111 (-57.1 %)	1519 (-41.3 %)	1444 (-44.2 %)	2587[c]
9.	CO_2	1506 (-34.5 %)	1109 (-51.8 %)	1159 (-49.6 %)	1417 (-38.4 %)	1511 (-34.3 %)	2300[g]
10.	N_2	793 (-27.9 %)	340 (-69.1 %)	534 (-51.4 %)	791 (-28.1 %)	759 (-31.0 %)	1100[e]
11.	NO	886 (-50.7 %)	353 (-80.4 %)	249 (-86.2 %)	876 (-51.3 %)	780 (-56.7 %)	1800[e]
12.	O_2	391 (-67.4 %)	258 (-78.5 %)	191 (-84.1 %)	385 (-67.9 %)	419 (-65.1 %)	1200[g]
13.	H_2S	1727 (-37.0 %)	971 (-64.6 %)	1305 (-52.4 %)	1662 (-39.4 %)	1598 (-41.7 %)	2743[c,k]
14.	CH_3CCH	2266 (-9.3 %)	1548 (-38.1 %)	1675 (-33.0 %)	2175 (-13.0 %)	2083 (-16.7 %)	2500 ± 40[h]
15.	HNCO	2046 (-47.5 %)	1376 (-64.7 %)	1644 (-57.8 %)	3260 (-16.4 %)	2058 (-47.2 %)	3900[i]
16.	CH_4	469 (-51.2 %)	145 (-84.9 %)	265 (-72.5 %)	374 (-61.2 %)	401 (-58.4 %)	963[j]
Average abs deviation		± 41.6 %	± 64.7 %	± 58 %	± 41.9 %	± 44.1 %	—
Frac. RMS deviation		0.435	0.659	0.597	0.443	0.456	—

Notes. Percentage deviation from experimental BE values (column 8) are shown in parentheses for columns 3, 4, 5, 6, and 7.
[a] Ward et al. (2012), [b] Olanrewaju et al. (2011), [c] Collings et al. (2004), [d] Dulieu et al. (2013), [e] Wakelam et al. (2017), [g] Minissale et al. (2016), [h] Kimber et al. (2014), [i] Noble et al. (2015), [j] Raut et al. (2007), [k] UMIST database (`http://udfa.ajmarkwick.net`).

Table 3. Calculated BEs using water hexamer (adsorbent) to check the effect of basis set superposition error (BSSE) using counterpoise method.

Sl. No.	Species	BE in Kelvin using MP2/aug-cc-pVDZ method	
		Values without BSSE correction	BSSE corrected values
1.	OCS	1808 (-25.5 %)	1294 (-46.7 %)
2.	HCl	4104 (-20.6 %)	3777 (-26.9 %)
3.	CH_3CN	3786 (-19.1 %)	2194 (-53.1 %)
4.	H_2O_2	5286 (-11.9 %)	4161 (-30.6 %)
5.	CH_3OH	4511 (-9.7 %)	3550 (-29.0 %)
6.	NH_3	5163 (-6.6 %)	3082 (-44.2 %)
7.	CO	1292 (-0.6 %)	840 (-35.3 %)
8.	C_2H_2	2640 (2.0 %)	1890 (-26.9 %)
9.	CO_2	2352 (2.2 %)	1624 (-29.3 %)
10.	N_2	1161 (5.5 %)	568 (-48.3 %)
11.	NO	1988 (10.4 %)	911 (-49.3 %)
12.	O_2	1352 (12.6 %)	519 (-56.7 %)
13.	H_2S	3232 (17.8 %)	1954 (-28.8 %)
14.	CH_3CCH	3153 (26.1 %)	1382 (-44.7 %)
15.	HNCO	5554 (42.4 %)	5017 (28.6 %)
16.	CH_4	1491 (54.8 %)	653 (-32.1 %)
Average absolute deviation		± 16.7 %	± 34.6 %
Fractional RMS deviation		0.221	0.395

Notes. Percentage deviation from experimental BE values are shown in parentheses for columns 3 and 4.

Table 4. Calculated BEs using water tetramer (adsorbent) to check the effect of higher order quantum chemical method.

Sl. No.	Species	BE in Kelvin using water tetramer	
		MP2/aug-cc-pVDZ	CCSD(T)/aug-cc-pVTZ
1.	N	269	273
2.	O	1002	1024
3.	O_2	940	853
4.	H_2O	2670	2632
5.	CO	1263	1196
6.	N_2	900	854

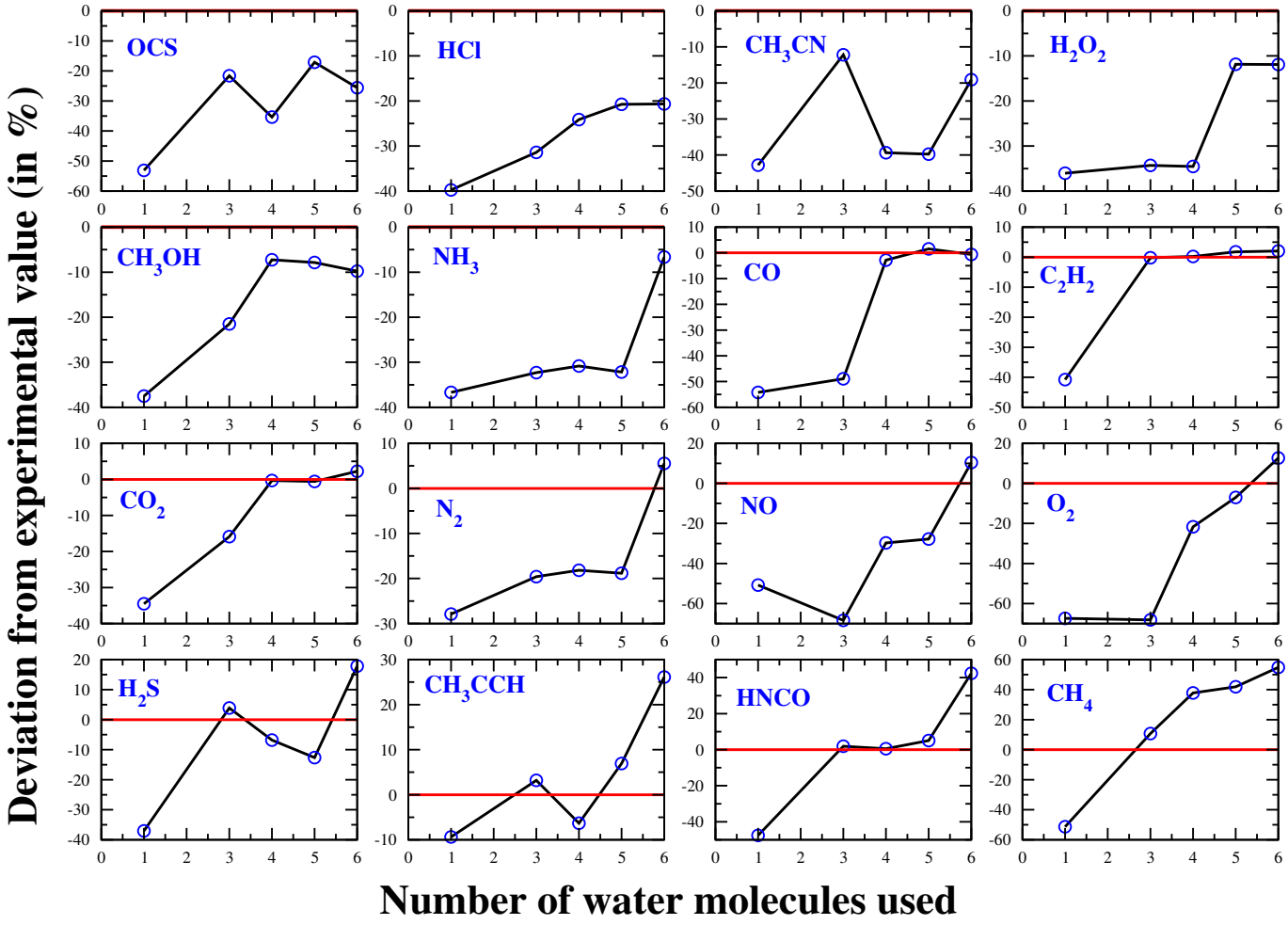


Figure 2. Percentage deviation of BEs of 16 stable species with increasing number of water clusters acting as the grain surface.

(2017)) which on an average deviate the results ±15.8% and ±16.7% respectively. Since, the calculations performed with c-pentamer and c-hexamer (chair) configurations can roughly estimate the experimental values, in the absence of the experimental values it is suggested to use these configurations. In Table 2, we have shown a comparison between the results obtained by considering BSSE corrections using counterpoise method (column 5 of Table 2) and without BSSE corrections (column 3 of Table 2) with water monomer. Considering water c-hexamer (chair) structure, same comparison is performed in Table 3. BSSE corrected BE values are found to be lower than that of without BSSE correction which imply that the basis set leads to significant BSSE. We have also shown the comparison between the results obtained by including ZPE (column 4 of Table 2) and without inclusion of ZPE (column 3 of Table 2) in case of only water monomer. It is to be noted that results obtained without inclusion of ZPE and BSSE corrections are

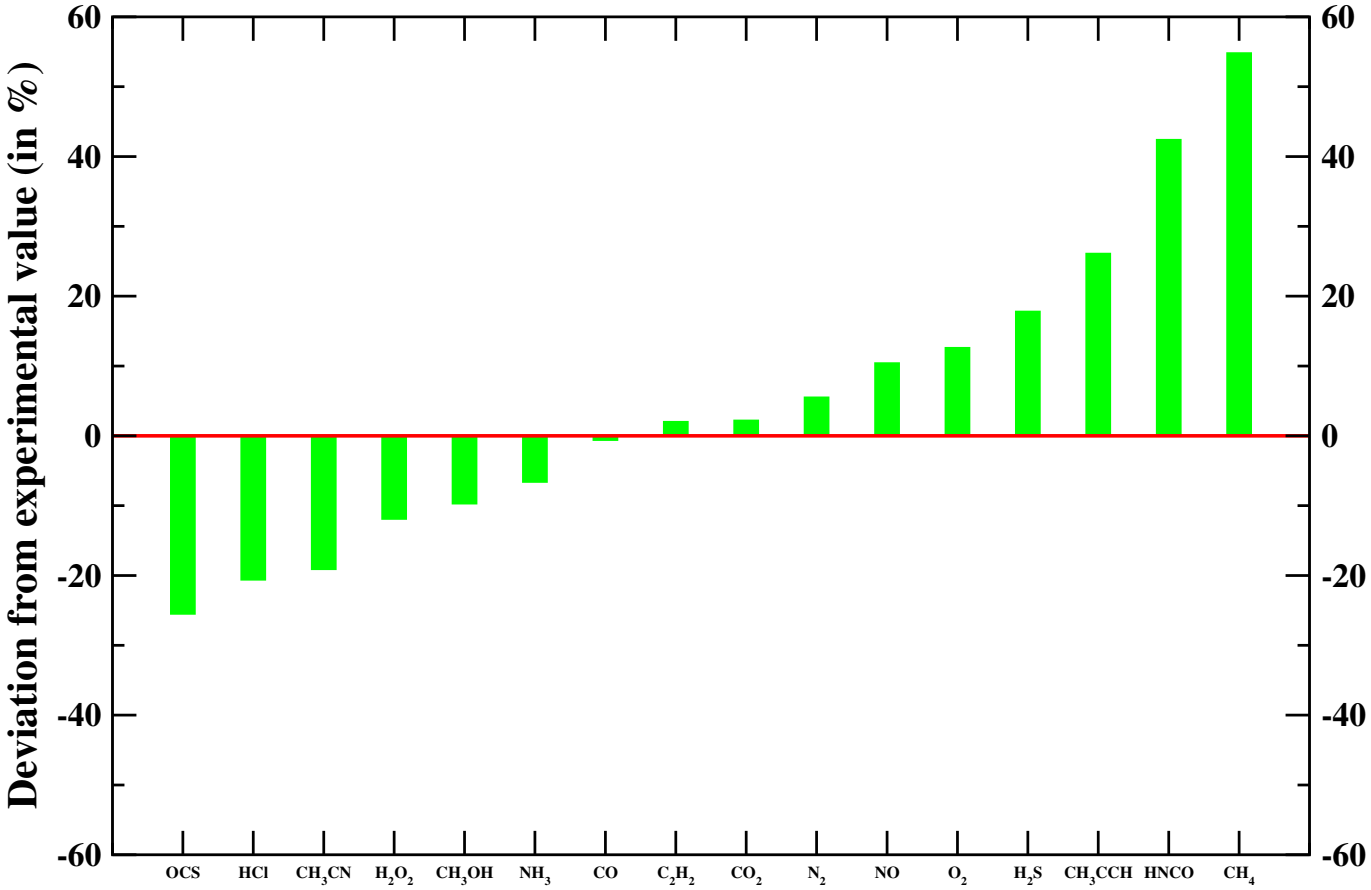


Figure 3. Percentage deviation from experimental BE values of 16 stable species using water c-hexamer (chair) cluster.

more closer to the experimental values. Also we have tested our BE calculations with water monomer by using higher level method and larger basis set (CCSD(T)/aug-cc-pVTZ) by single point energy calculation (column 7 of Table 2). We show in Table 4 the BE calculations of some selected species (N, O, O_2, H_2O, CO and N_2) with water tetramer using higher method and basis set (CCSD(T)/aug-cc-pVTZ). We found a minor change with these considerations except the effect of ZPE though in Wakelam et al. (2017) case, the ZPE effect is small because the ZPE is roughly proportional to the BE and after inclusion of the ZPE the parameters for the fits are not the same but the result of the fits show similar deviation. However, we noticed that among all the methods or basis sets used in our computation, MP2 method with aug-cc-pVDZ basis set (without considering ZPE and BSSE corrections) stands comparatively best with respect to the experimental values. The fact that a low level of theory (small basis set, no BSSE correction, no ZPE) results is in better agreement with experiment than a higher level is likely due to the fact that the various approximations at low level compensate each other. This is probably a coincidence, but is useful at it makes it easier to process a large number of systems.

BE calculations with water pentamer and hexamer configurations is very time consuming and thus it is difficult to apply for a large set of species. In Appendix (Table A1), we provide our calculated BE values for 21 species with c-hexamer (chair) configuration. Since BE values taking water c-hexamer (chair) cluster configuration deviate by $\sim \pm 16.7\%$, they can be scaled by 1 ± 0.167. We also provide our calculated BE values for a large set of 100 important interstellar or circumstellar species, where, we consider the c-tetramer configuration (as given in Fig. 1) of water cluster as a substrate (which deviates the experimental values by $\sim \pm 18.8\%$) and BE values of these species can also be scaled by 1 ± 0.188. We think that our calculations for the tetramer is an interesting alternative to full calculation or to the fitting model used by Wakelam et al. (2017). Some strange values of BE of some species are due to induce deviation for the global minimum. The mobility of atoms is very important for grain chemistry in dense molecular

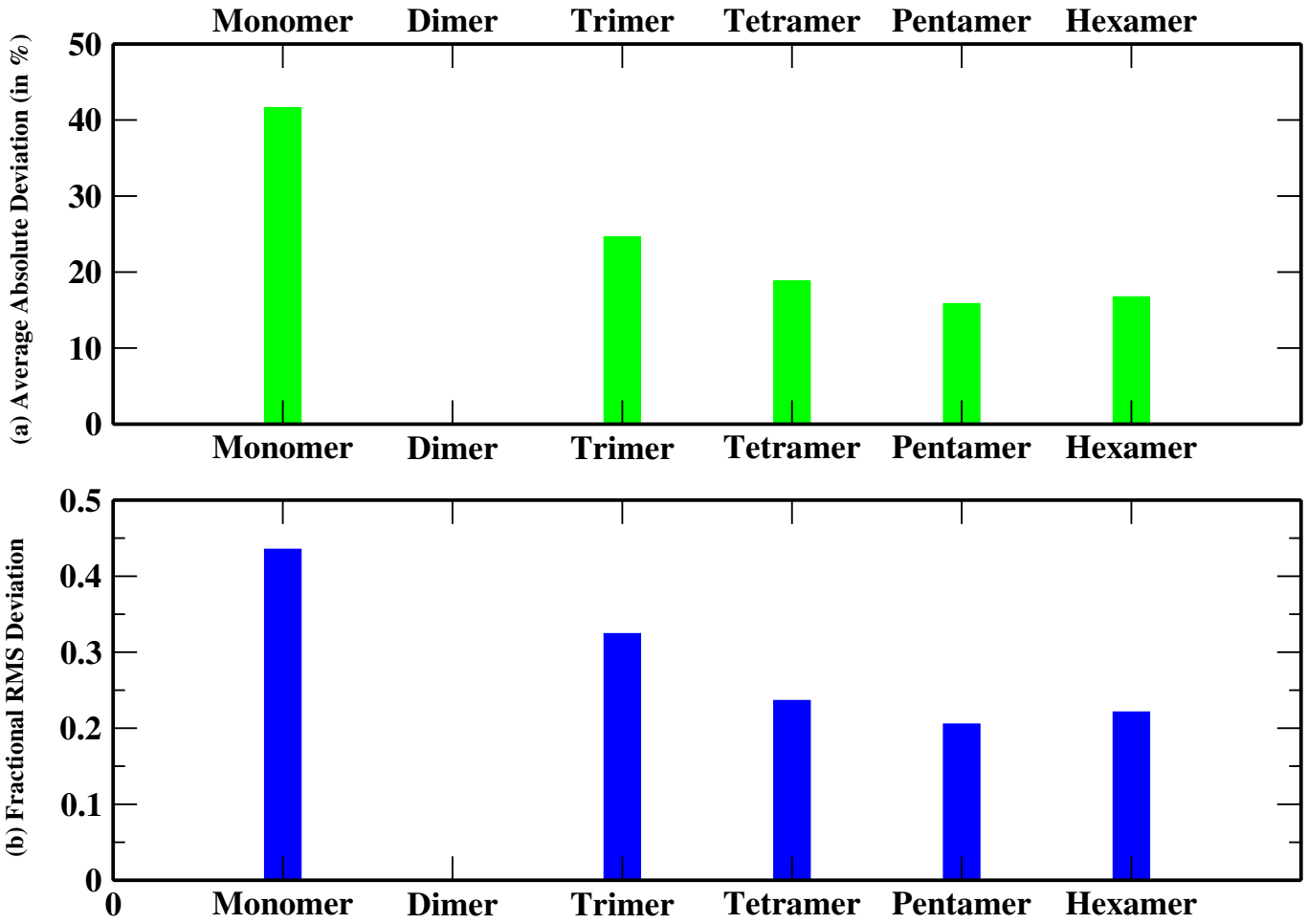


Figure 4. (a) Average absolute percentage deviation and (b) fractional RMS deviation of our calculated values from experiment.

clouds which depend mostly on their adsorption energy with grain surface. BEs of some relevant atoms (such as H, He, C, N, O, Na, Mg, Si, P, and S) are also included in Table A1. With the tetramer configuration, our calculations likely deviate the experimental BE values due to the long-range interaction (interaction with water molecule not close to the species as visible from Fig. A3(a-e) which seems crucial for the cases of low BEs. So, using only a scale factor without offset with the tetramer configuration may likely underestimate the real BE, particularly for low BE cases.

Previously used and recently proposed KIDA (`http://kida.obs.u-bordeaux1.fr`) BE values by Wakelam et al. (2017) and BE values provided by other sources are given in columns 6, 7 and 8 respectively of Table A1. Among the sixteen stable species given in Table 1 and 2, there are both polar (OCS, CH_3OH, NH_3, H_2S, CH_3CCH, CH_3CN, H_2O_2, HCl, HNCO, NO) and non-polar molecules (CO, CO_2, N_2, O_2, CH_4, C_2H_2).We have noticed that for the non-polar species if we choose the position at the center of water cluster, our calculation sometimes overestimates the attractive interaction. For species (like HCl, CH_3OH, etc.) leading to hydrogen bond with H_2O, the species is rather localized on one water molecule with H-bonding and in most of the cases, the interaction is well reproduced by our calculations. We found the case of oxygen atom as an intermediate one. We have obtained the BE of oxygen atom to be 1002 K and 660 K (given in Table A1) respectively with the tetramer and c-hexamer (chair) configuration whereas the existing value was 1660 ± 60 K in KIDA desorption energy on ASW surface. This is because of the complex containing water c-hexamer (chair) with oxygen atom is notably modified and so the interaction between water is less good and it seems that this is not compensated by the interaction with the oxygen atom. But in the case of the complex containing water tetramer with oxygen atom gives more accurate value likely because in that case water interaction is not so perturbed. The hydrogen atom case (125 K with tetramer and 181 K with hexamer from Table A1) is a very strange one as it leads to a much smaller interaction in comparison to the value (= 650 K) mentioned in Al-Halabi & van

Dishoeck (2007). Thus, though we are having very good approximation (on an average) by using the c-pentamer and c-hexamer (chair) configuration, we should keep in mind that using only one adsorption site geometry may induce notable error on BE. For a given method and for a given species, it is recommended to consider various adsorption sites and various stable geometries and take an average value to come up with a more relevant approximation. In our case, when various binding sites where found, we try to choose the closest one with previous calculations. In Figs. A1, A2, and A3(a-e) of the appendix, we provide our optimized geometries for the species considered here with c-hexamer (chair), c-pentamer, and c-tetramer configurations respectively. Used ground states of each species are also provided in column 3 of Table A1.

4. CONCLUSIONS

In this work, we compute BE of various interstellar species on water surface. We performed a systematic quantum chemical calculations for various adsorbed species by considering water monomer, c-trimer, c-tetramer, c-pentamer, and c-hexamer (chair) configuration respectively as a substrate to investigate the physisorption BE of species. The advantage of using two or more water molecules is that one can take into account the H bonding donor and acceptor behaviour of some molecules. We noticed that our calculated values of BE tend to experimental values with increasing cluster size of water molecules which is very clear from calculated absolute average percentage deviation and root mean square deviation values given in Table 1. More specifically, when we considered the c-pentamer and c-hexamer (chair) configurations, on an average, our computed BE values deviate with experimental values within of $\sim \pm 15.8\%$ and $\sim \pm 16.7\%$ respectively. The results obtained using a low level of theory (small basis set, no BSSE correction, no ZPE) is in better agreement with experiment than a higher level likely due to the fact that the various approximations at low level compensate each other. This is probably a coincidence, but is useful as it makes it easier to process a large number of systems. For a wide set of interstellar or circumstellar species, we provide the BE values with the c-tetramer configuration which are deviated by on an average of $\sim \pm 18.8\%$. These comparisons show that we can safely use our procedure to compute BE of any such molecules with reasonable accuracy.

5. ACKNOWLEDGEMENT

MS gratefully acknowledges DST, the Government of India for providing financial assistance through DST-INSPIRE Fellowship [IF160109] scheme. AD and PG acknowledge ISRO respond project (Grant No. ISRO/RES/2/402/16-17) for partial financial support.

Software: Gaussian 09 (Frisch et al. 2013)

REFERENCES

Al-Halabi, A., & van Dishoeck, E.F. 2007, MNRAS, 382, 1648

Chakarov, D., & Kasemo, B. 1998, PhRvL, 81, 5181

Charnley, S.B. 1997, MNRAS, 291, 455

Collings, M.P., Anderson, M.A., Chen, R., et al. 2004, MNRAS, 354, 1133

Chaabouni, H., Diana, S., Nguyen, T., Dulieu, F. 2018, A&A, doi: https://doi.org/10.1051/0004-6361/201731006

Das, A., Acharyya, K. & Chakrabarti, S.K. 2010, MNRAS, 409, 789

Das, A. & Chakrabarti, S.K. 2011, MNRAS, 418, 545

Das, A., Sahu, D., Majumdar, L., & Chakrabarti, S.K. 2016, MNRAS, 455, 540

Dulieu, F., Congiu, E., Noble, J., et al. 2013, NatSR, 3, 1338

Dunning Jr, T.H. 1989, JChPh, 90(2), 1007

Frisch, M. J., Trucks, G. W., Schlegel, H. B., et al. 2013, Gaussian 09, Revision D.01, Gaussian, Inc., Wallingford CT.

Garrod, R.T., & Herbst, E. 2006, A&A, 457, 927

Garrod, R.T., Wakelam, V., & Herbst, E. 2007, A&A, 467, 1103

Gorai, P., Das, A., Das, A., Sivaraman, B., et al. 2017, ApJ, 836,70

Gorai, P., Das, A., Majumdar. L., et al. 2017, MolAp, 6, 36-46

Hama, T., & Watanabe, N. 2013, ChRv, 113, 8783

Hasegawa, T.I., & Herbst, E. 1993, MNRAS, 263, 589

Herbst, E.; van Dishoeck, E. F. Annu. Rev. Astron. Astrophys. 2009, 47, 427

He, J., Shi, J., Hopkins, T., Vidali, G., & Kaufman, M.J. 2015, ApJ, 801(2), 120

Hornekr, L., Baurichter, A., Petrunin, V.V., et al. 2005, JChPh, 122(12), 124701

Karssemeijer, L.J., & Cuppen, H.M. 2014, A&A, 569, A107

Keane J.V., Tielens A.G.G.M., Boogert A.C.A., Schutte W.A., & Whittet D.C.B. 2001, A&A, 376, 254

Kimber, H.J., Ennis, C.P., & Price, S.D. 2014, FaDi, 168, 167

Lamberts, T., & Kästner, J. 2017, ApJ, 846(1), 43

Maldoni, M.M., Egan, M.P., Smith, R.G., Robinson, G., & Wright, C.M. 2003, MNRAS, 345, 912

Malfait, K., Waelkens, C., Waters, L.B.F.M., et al. 1998, A&A, 332, L25

Minissale, M., & Dulieu, F. 2014, JChPh, 141, 014304

Minissale, M., Dulieu, F., Cazaux, S., & Hocuk, S. 2016, A&A, 585, A24

Noble, J. A., Congiu, E., Dulieu, F., & Fraser, H. J. 2012, MNRAS, 421(1), 768

Noble, J.A., Theule, P., Congiu, E., et al. 2015, A&A, 576, A91

Ohno, K., Okimura, M., Akaib, N., & Katsumotoa, Y. 2005, PCCP, 7, 3005

Olanrewaju, B.O., Herring-Captain, J., Grieves, G.A., Aleksandrov, A., & Orlando, T.M. 2011, JPCA, 115, 5936

Palumbo, M.E. 2006, A&A, 453, 903

Penteado, E.M., Walsh, C., & Cuppen, H.M. 2017, ApJ, 844(1), 71

Raut, U., Fam, M., Teolis, B.D., et al. 2007, JChPh, 127, 204713

Ruaud, M., Loison, J.C., Hickson, K.M., et al. 2015, MNRAS, 447(4), 4004

Shimonishi, T., Nakatani, N., Furuya, K., & Hama, T. 2018, arXiv preprint, arXiv:1801.08716.

Sil, M., Gorai, P., Das, A., et al. 2018, ApJ, 853, 2,

Sil, M., Gorai, P., Das, A., Sahu, D., & Chakrabarti, S.K. 2017, EPJD, 71, 45

Song, L., & Kästner, J. 2016, PCCP, 18(42), 29278

Tielens, A.G.G.M., & Hagen, W. 1982, A&A, 114, 245

Wakelam, V., Loison, J.-C., Mereau, R., & Ruaud, M. 2017, MolAs, 6, 22

Ward, M.D., Hogg, I.A., & Price, S.D. 2012, MNRAS, 425, 1264

Williams, D. & Herbst, E. 2002, SurSc, 500, 823

Whittet, D.C.B., Bode, M.F., Longmore, A.J., et al. 1988, MNRAS, 233, 321

Appendix

Table A1: Calculated and Available list of BEs of Various Species.

Serial Number	Species	Ground state used	BE in Kelvin on water tetramer	BE in Kelvin on water hexamer	BE from KIDA database		BE in Kelvin from other literature sources
					Old values (Kelvin)	New values (Kelvin)	
1.	H	Doublet	125	181	450[g]	650 ± 195	650 ± 100[c]
2.	H_2	Singlet	528	545	450	440 ± 132	500 ± 100[c]
3.	He	Singlet	113		100		100 ± 50[c]
4.	C	Triplet	660		800	10000 ± 3000	715 ± 360[c], 14100 ± 420[k]
5.	N	Quartet	269	619	800	720 ± 216	715 ± 358[c], 400 ± 30[k]
6.	O	Triplet	1002	660	1660 ± 60[a]	1600 ± 480	1660 ± 60[c], 1504 ± 12[j], 1440 ± 160[k]
7.	Na	Doublet	2214		11800		10600 ± 500[c]
8.	Mg	Singlet	654		5300		4750 ± 500[c]
9.	Si	Triplet	6956		2700	11600 ± 3480	2400 ± 500[c]
10.	P	Quartet	616		1100		750 ± 375
11.	S	Triplet	1428		1100	2600 ± 780	985 ± 495[c]
12.	NH	Triplet	1947		2378	2600 ± 780	542 ± 270[c]
13.	OH	Doublet	3183		2850[g]	4600 ± 1380	3210 ± 1550[c]
14.	PH	Triplet	944				800 ± 400
15.	C_2	Triplet	9248		1600		1085 ± 500[c]
16.	HF	Singlet	5540				500 ± 250
17.	HCl	Singlet	3924	4104	5174 ± 1[b]	5172 ± 1551.6	900 ± 450
18.	CN	Doublet	1736		1600		1355 ± 500[c]
19.	N_2	Singlet	900	1161	1000[g]	1100 ± 330	990 ± 100[c], 1000[f]
20.	CO	Singlet	1263	1292	1150[g]	1300 ± 390	1100 ± 250[c], 1300[e]
21.	SiH	Doublet	8988		3150	13000 ± 3900	2620 ± 500[c]
22.	NO	Doublet	1265	1988	1600	1600 ± 480	1085 ± 500[c]
23.	O_2	Triplet	940	1352	1000	1200 ± 360	898 ± 30[c], 1200[e], 1000[f]
24.	HS	Doublet	2221		1450	2700 ± 810	1350 ± 500[c]
25.	SiC	Triplet	5850		3500		3150 ± 500[c]
26.	CP	Doublet	1699		1900		1050 ± 500
27.	CS	Singlet	2217		1900	3200 ± 960	1800 ± 500[c]
28.	NS	Doublet	2774		1900		1800 ± 500[c]
29.	SO	Triplet	2128		2600	2800 ± 840	1800 ± 500[c]
30.	S_2	Triplet	1644		2200		2000 ± 500[c]
31.	CH_2	Triplet	1473		1050	1400 ± 420	860 ± 430[c]
32.	NH_2	Doublet	3240		3956	3200 ± 960	770 ± 385[c]
33.	H_2O	Singlet	2670	4166	5700[g]	5600 ± 1680	4800 ± 100[c]
34.	PH_2	Doublet	1226		2000		850 ± 425
35.	C_2H	Doublet	2791		2137	3000 ± 900	1330 ± 500[c]
36.	N_2H	Doublet	3697		1450		
37.	O_2H	Doublet	5778		3650	5000 ± 1500	1510 ± 500[c]
38.	HS_2	Doublet	4014		2650		2300 ± 500[c]
39.	HCN	Singlet	2352		2050	3700 ± 1110	1580 ± 500[c]
40.	HNC	Singlet	5225		2050	3800 ± 1140	1510 ± 500[c]
41.	HCO	Doublet	1857		1600[g]	2400 ± 720	1355 ± 500[c]
42.	HOC	Doublet	5692				
43.	HCS	Doublet	2713		2350	2900 ± 870	2000 ± 500[c]
44.	HNO	Singlet	2988		2050	3000 ± 900	1510 ± 500[c]
45.	H_2S	Singlet	2556	3232	2743[f]	2700 ± 810	2290 ± 90[c]
46.	C_3	Singlet	2863		2400	2500 ± 750	2010 ± 500[c]
47.	O_3	Singlet	2545		1800	2100 ± 630	2100 ± 100[c]
48.	C_2N	Doublet	1281		2400		2010 ± 500[c]
49.	C_2S	Triplet	2477		2700		2500 ± 500[c]
50.	OCN	Doublet	3085		2400		1805 ± 500[c]

Serial Number	Species	Ground state used	BE in Kelvin on water tetramer	BE in Kelvin on water hexamer	BE from KIDA database		BE in Kelvin from other literature sources
					Old values (Kelvin)	New values (Kelvin)	
51.	CO_2	Singlet	2293	2352	2575	2600 ± 780	2267 ± 70[c], 2300[e]
52.	OCS	Singlet	1571	1808	2888	2400 ± 720	2325 ± 95[c]
53.	SO_2	Singlet	3745		3405	3400 ± 1020	3010 ± 110[c]
54.	CH_3	Doublet	1322		1175	1600 ± 480	1040 ± 500[c]
55.	NH_3	Singlet	3825	5163	5534	5500 ± 1650	2715 ± 105[c], 5530[f]
56.	SiH_3	Doublet	1269		4050		3440 ± 500[c]
57.	C_2H_2	Singlet	2593	2640	2587[f]	2587 ± 776.1	2090 ± 85[c]
58.	N_2H_2	Singlet	3183				
59.	H_2O_2	Singlet	3928	4248	5700	6000 ± 1800	6000 ± 100[c], 5410[l]
60.	H_2S_2	Singlet	4368		3100		2600 ± 500[c]
61.	H_2CN	Doublet	2984		2400		2400 ± 500[c]
62.	CHNH	Doublet	3742				
63.	H_2CO	Singlet	3242		2050[g]	4500 ± 1350	3260 ± 60[c]
64.	CHOH	Triplet	4800				
65.	HC_2N	Triplet	3289				2270 ± 500[c]
66.	HC_2O	Doublet	2914		2400		2010 ± 500[c]
67.	HNCO	Singlet	3922	5554	2850	4400 ± 1320	2270 ± 500[c], 3900[h]
68.	H_2CS	Singlet	3110		2700	4400 ± 1320	2025 ± 500[c]
69.	C_3O	Singlet	3542		2750		2520 ± 500[c]
70.	CH_4	Singlet	1327	2321	1300[g]	960 ± 288	1250 ± 120[c]
71.	SiH_4	Singlet	1527		4500		3690 ± 500[c]
72.	C_2H_3	Doublet	2600		3037	2800 ± 840	1760 ± 500[c]
73.	$CHNH_2$	Triplet	1681				
74.	CH_2NH	triplet	3354		5534		1560 ± 500[c]
75.	CH_3N	Triplet	2194				
76.	c-C_3H_2	Singlet	3892		3387	5900 ± 1770	2110 ± 500[c]
77.	H_2CCN	Doublet	3730		4230		2470 ± 500[c]
78.	H_2CCO	Singlet	2847		2200	2800 ± 840	2520 ± 500[c]
79.	HCOOH	Singlet	3483		5570[g]		4532 ± 150[c]
80.	CH_2OH	Doublet	4772		5084	4400 ± 1320	2170 ± 500[c]
81.	NH_2OH	Singlet	4799				2770 ± 500[c]
82.	C_4H	Doublet	2946		3737		2670 ± 500[c]
83.	HC_3N	Singlet	2925		4580		2685 ± 500[c]
84.	HC_3O	Doublet	2619				
85.	C_5	Singlet	2403		4000		3220 ± 500[c]
86.	C_2H_4	Singlet	2052		3487	2500 ± 750	2010 ± 500[c]
87.	CH_2NH_2	Doublet	3831		5534[d]		
88.	CH_3NH	Doublet	3414				1760 ± 500[c]
89.	CH_3OH	Singlet	4368	4511	5534	5000 ± 1500	3820 ± 135[c], 5530[f]
90.	CH_2CCH	Doublet	2726		3837	3300 ± 990	3840 ± 500[c]
91.	CH_3CN	Singlet	2838	3786	4680[f]	4680 ± 1404	3790 ± 130[c]
92.	H_2C_3N	Doublet	2637				
93.	H_2C_3O	Singlet	3006				
94.	C_6	Quintet	3226		4800		3620 ± 500[c]
95.	CH_3NH_2	Singlet	4434		6584		5130 ± 500[c], 4269[m]
96.	C_2H_5	Doublet	1752		3937	3100 ± 930	2110 ± 500[c]
97.	CH_3CCH	Singlet	2342	3153	4287	3800 ± 1140	4290 ± 500[c], 2500 ± 40[i]
98.	CH_2CCH_2	Triplet	2705			3000 ± 900	4290 ± 500[c]
99.	CH_3CHO	Singlet	3849		2450	5400 ± 1620	2870 ± 500[c]
100.	C_7	Singlet	4178		5600		4430 ± 500[c]

Notes. Average deviation from experiment in case of tetramer (column 4) and hexamer (column 5) are ∼ ±18.8% and ∼ ±16.7% respectively.
[a] He et al. (2015), [b] Olanrewaju et al. (2011), [c] Penteado et al. (2017), [d] Ruaud et al. (2015), [e] Minissale et al. (2016), [f] Collings et al. (2004), [g] Garrod & Herbst (2006), [h] Noble et al. (2015), [i] Kimber et al. (2014), [j] Ward et al. (2012), [k] Shimonishi et al. (2018), [l] Lamberts et al. (2017). [m] Chaabouni et al (2018)

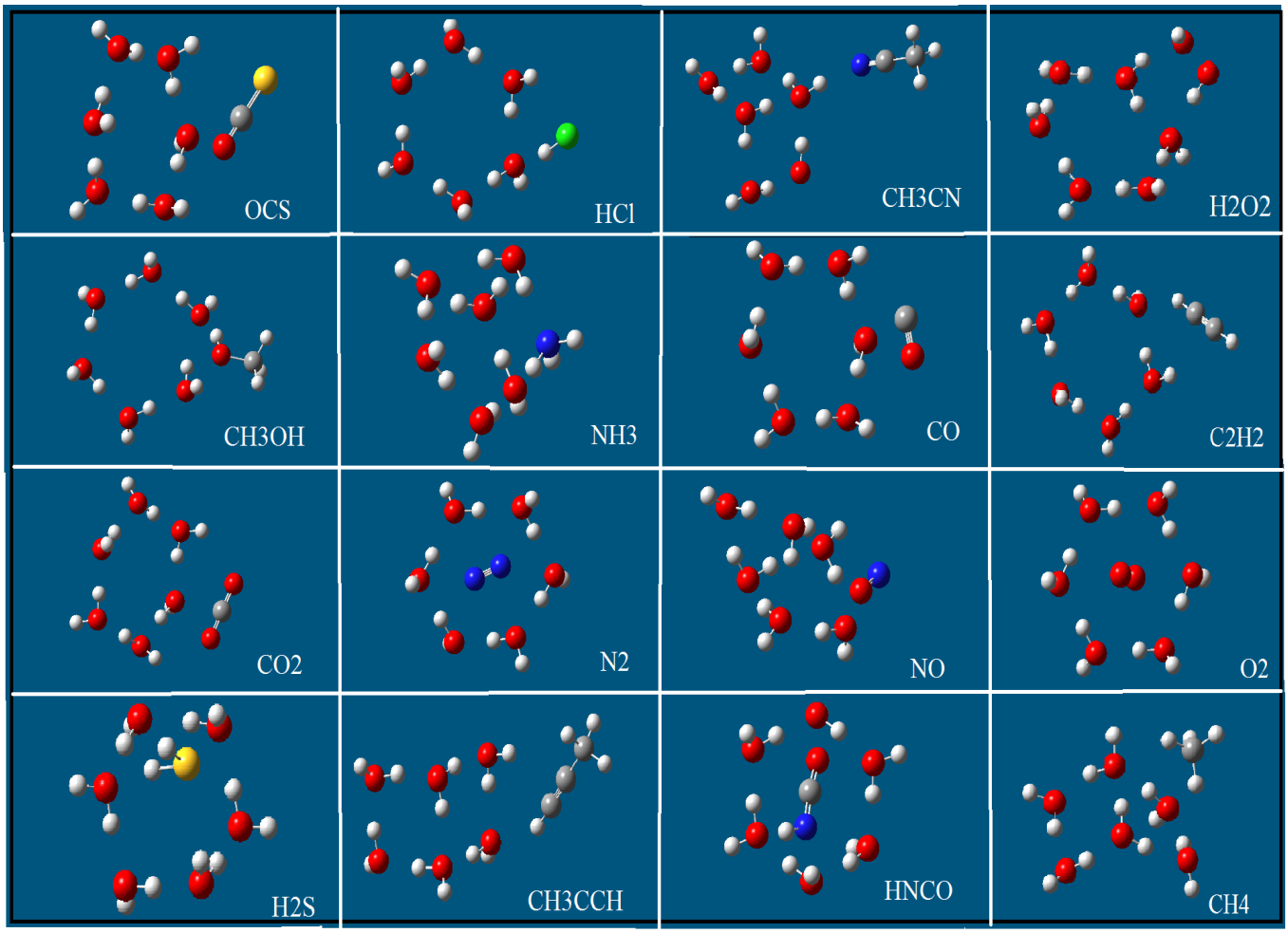


Figure A1. Optimized Geometries with the c-hexamer (chair) Configuration.

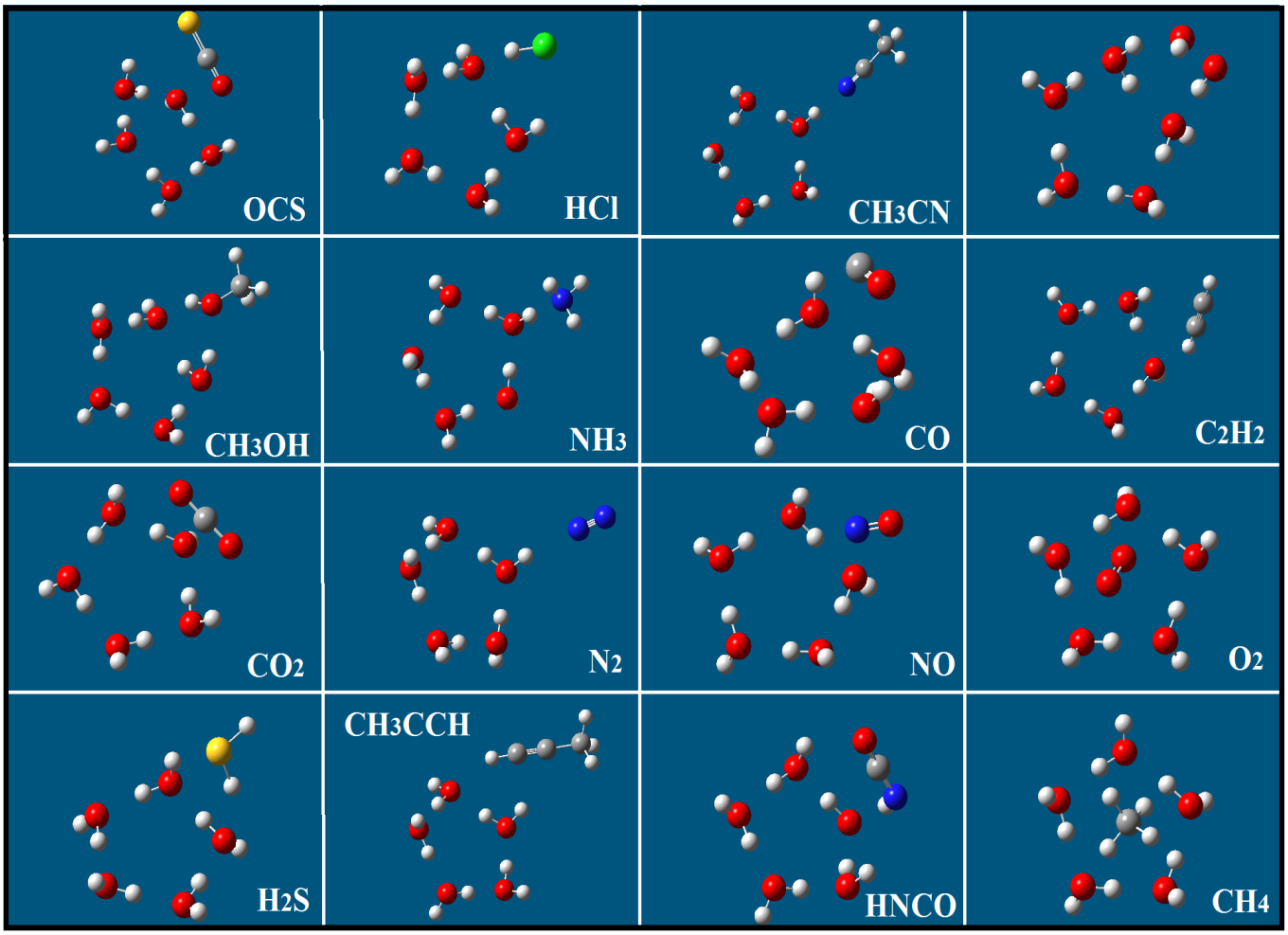


Figure A2. Optimized Geometries with the c-pentamer Configuration.

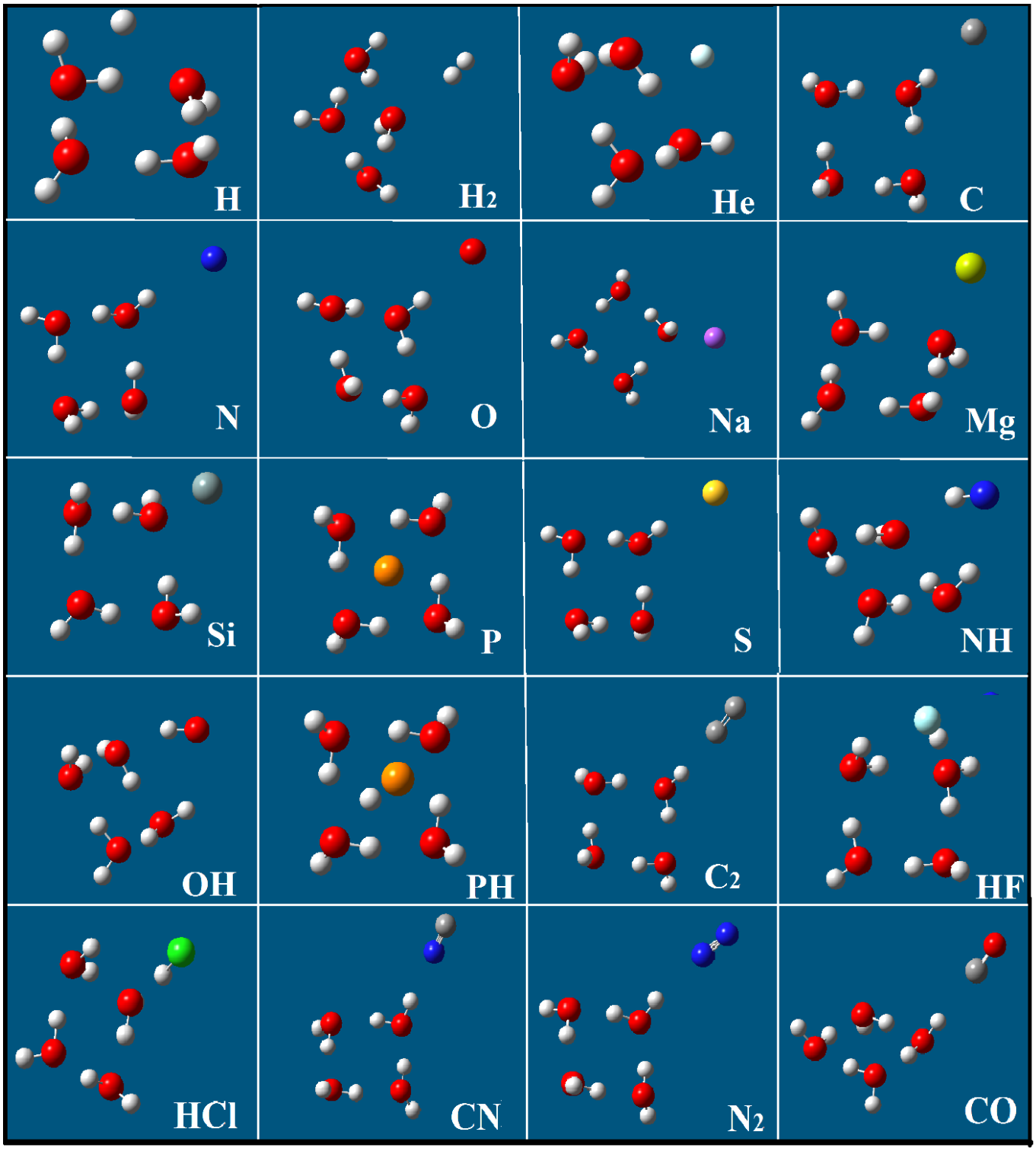


Figure A3(a). Optimized Geometries with the c-tetramer Configuration.

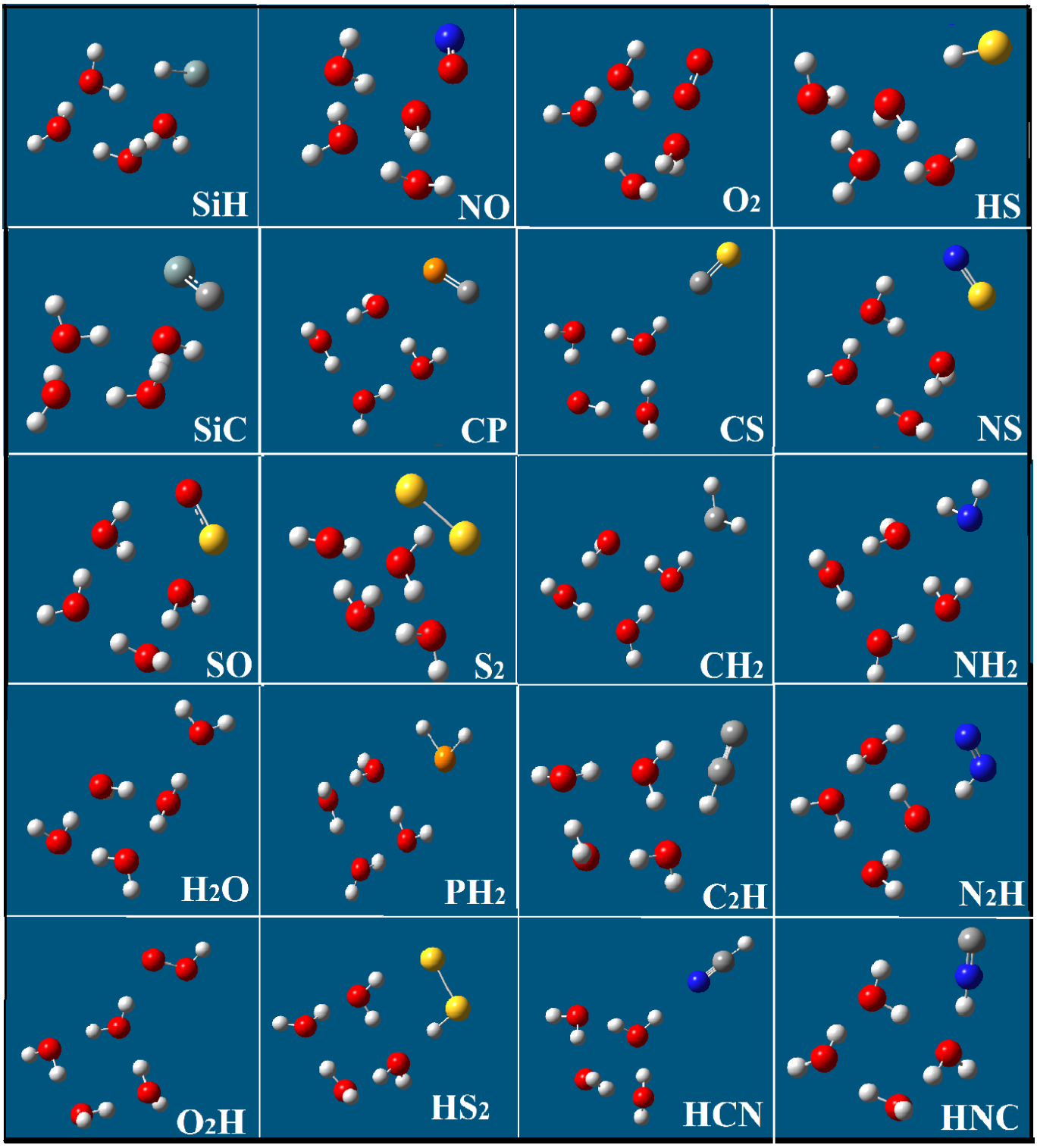


Figure A3(b). Optimized Geometries with the c-tetramer Configuration.

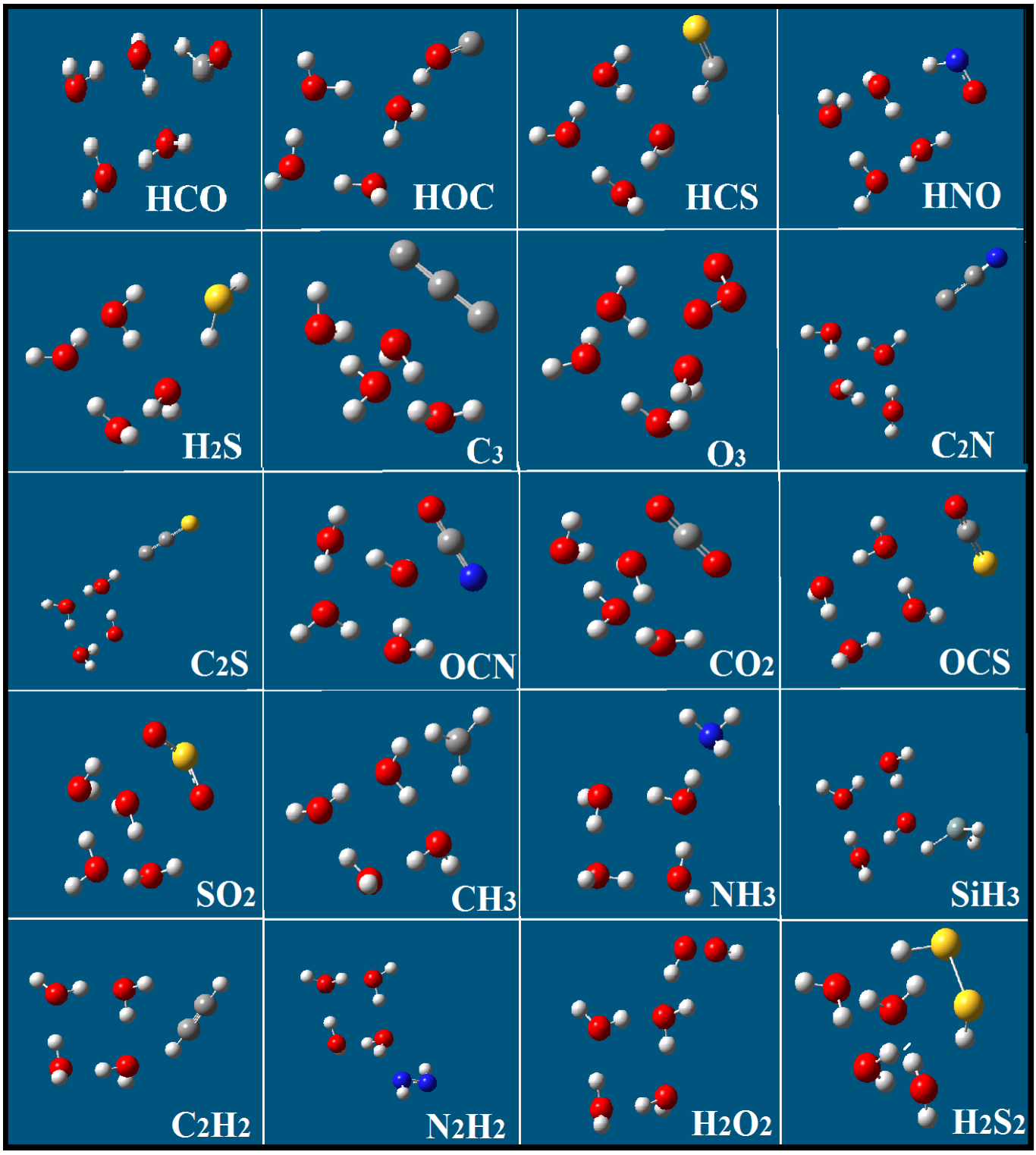


Figure A3(c). Optimized Geometries with the c-tetramer Configuration.

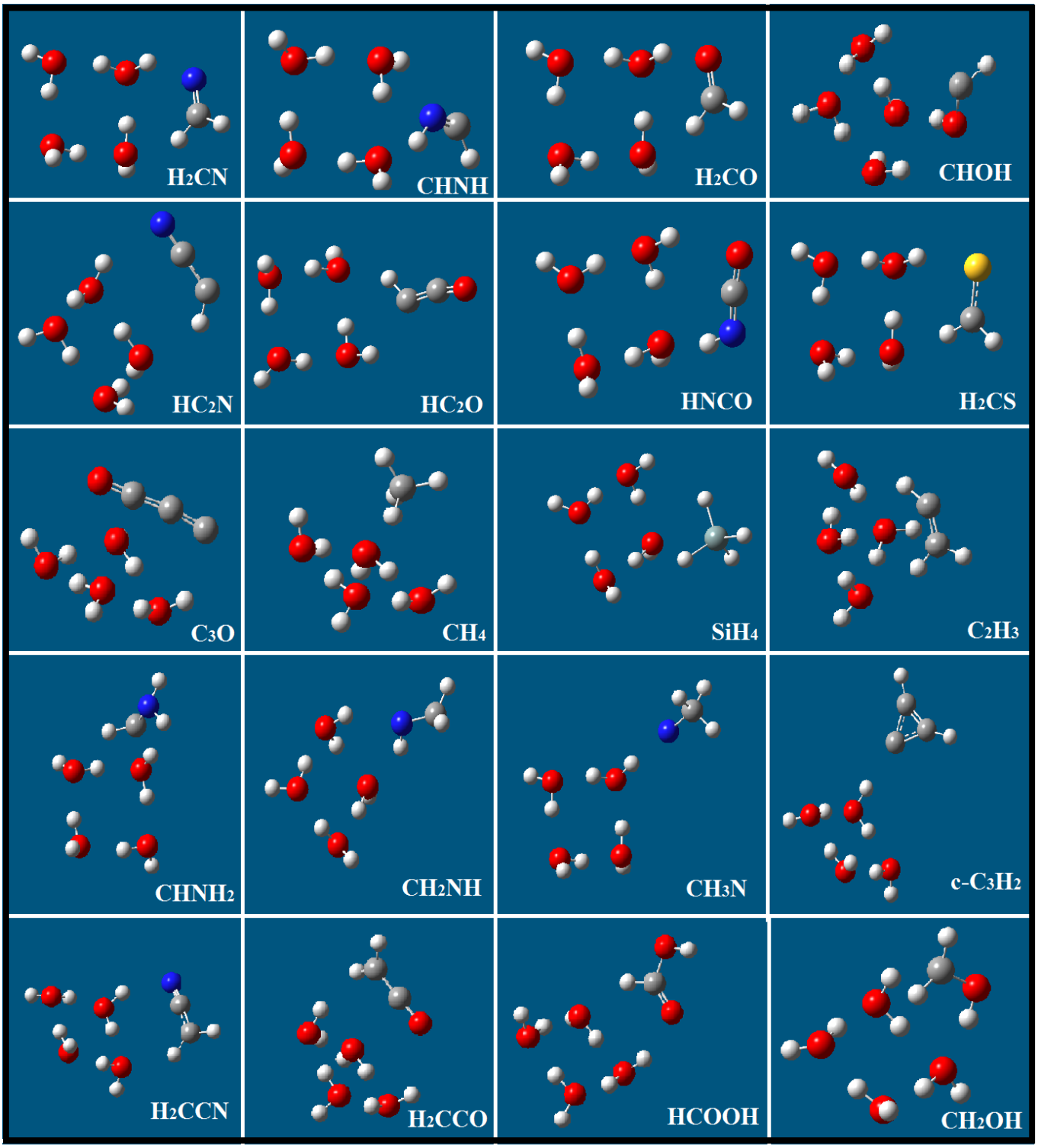


Figure A3(d). Optimized Geometries with the c-tetramer Configuration.

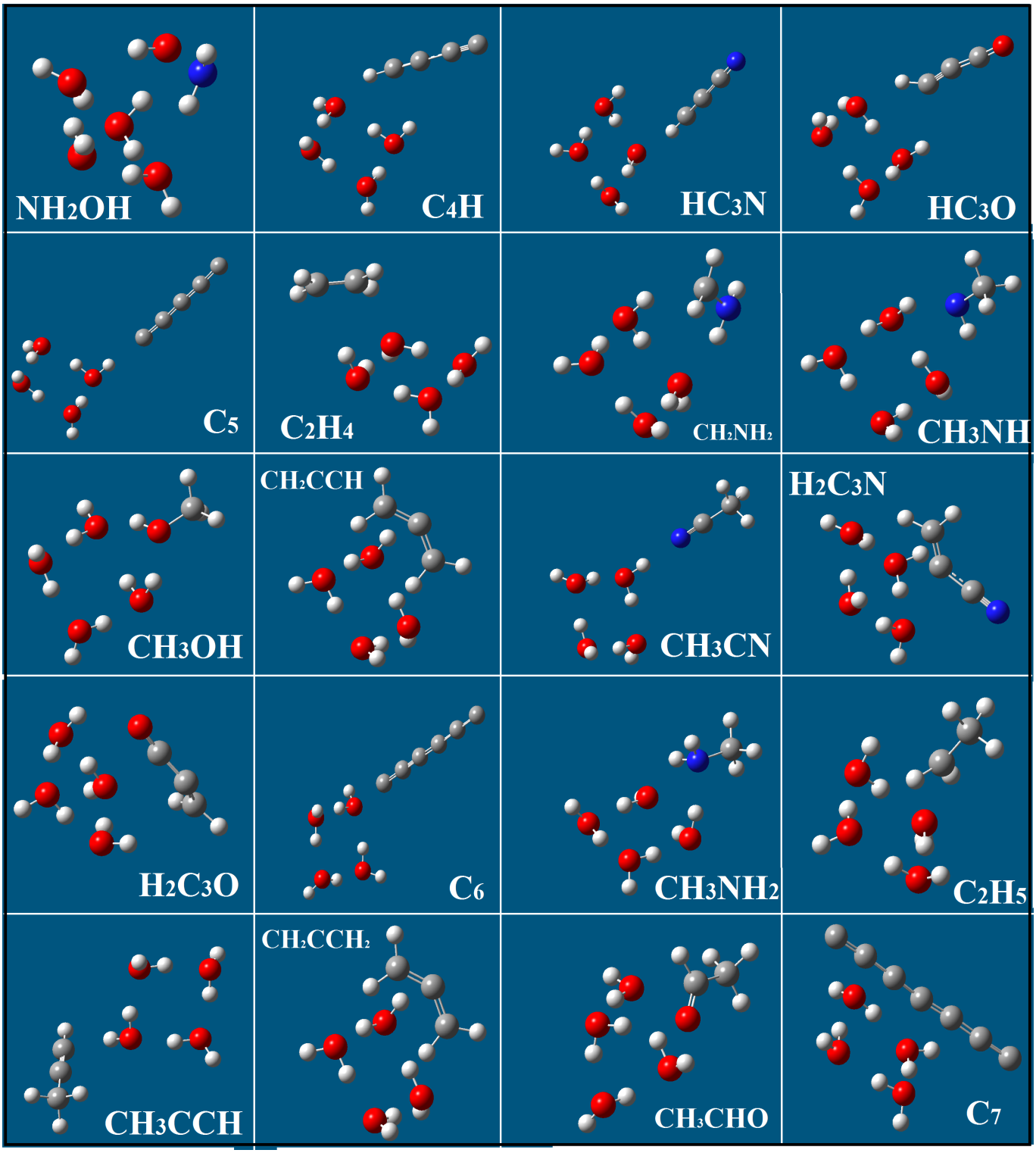


Figure A3(e). Optimized Geometries with the c-tetramer Configuration.